

Accepted Manuscript

Title: Estimation of differential heat of dilution for aqueous lithium (bromide, iodide, nitrate, chloride) solution and aqueous (lithium, potassium, sodium) nitrate solution used in absorption cooling systems

Author: Faisal Asfand, Mahmoud Bourouis

PII: S0140-7007(16)30252-3

DOI: <http://dx.doi.org/doi: 10.1016/j.ijrefrig.2016.08.008>

Reference: IJR 3405

To appear in: *International Journal of Refrigeration*

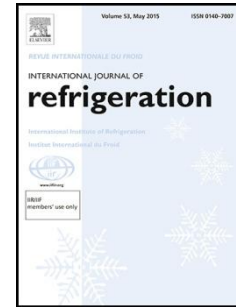
Received date: 18-3-2016

Revised date: 4-8-2016

Accepted date: 20-8-2016

Please cite this article as: Faisal Asfand, Mahmoud Bourouis, Estimation of differential heat of dilution for aqueous lithium (bromide, iodide, nitrate, chloride) solution and aqueous (lithium, potassium, sodium) nitrate solution used in absorption cooling systems, *International Journal of Refrigeration* (2016), <http://dx.doi.org/doi: 10.1016/j.ijrefrig.2016.08.008>.

This is a PDF file of an unedited manuscript that has been accepted for publication. As a service to our customers we are providing this early version of the manuscript. The manuscript will undergo copyediting, typesetting, and review of the resulting proof before it is published in its final form. Please note that during the production process errors may be discovered which could affect the content, and all legal disclaimers that apply to the journal pertain.



**Estimation of differential heat of dilution for aqueous lithium
(bromide, iodide, nitrate, chloride) solution and aqueous (lithium,
potassium, sodium) nitrate solution used in absorption cooling
systems**

Faisal Asfand, Mahmoud Bourouis*

Department of Mechanical Engineering – Universitat Rovira i Virgili,

Av. Països Catalans No. 26, 43007 Tarragona, Spain.

*Corresponding author

Email: mahmoud.bourouis@urv.cat ; Phone: +34 977 55 86 13 ; Fax: +34 977 55 96 91

Keywords: Differential heat of dilution, Duhring's diagram, Water/LiBr,
Water/(LiBr+LiI+LiNO₃+LiCl), Water/(LiNO₃+KNO₃+NaNO₃), Absorption cooling

Highlights

- 1) Differential heat of dilution was estimated theoretically from the vapour pressure data.
- 2) Estimated results for water/LiBr were in close agreement with the experimental results.
- 3) The differential heat of dilution data obtained were correlated with polynomial equations.
- 4) The correlations developed could be useful in performing heat and mass transfer analysis.

Abstract

The differential heat of dilution data are estimated theoretically using Duhring's diagrams for water/LiBr, water/(LiBr+LiI+LiNO₃+LiCl) with mass compositions in salts of 60.16%, 9.55%, 18.54% and 11.75%, respectively, and water/(LiNO₃+KNO₃+NaNO₃) with mass compositions in salts of 53%, 28% and 19%, respectively, as these can be potentially utilized as working fluids in absorption cooling systems. The differential heat of dilution data obtained were correlated with simple polynomial equations for the three working fluids as a function of the solution concentration and temperature. The results showed that the differential heat of dilution of the non-conventional working fluid mixtures is lower than that of water/LiBr at typical operating temperature and concentration of interest in absorption cooling cycles employing these working fluid mixtures. The correlations developed could be useful in predicting the differential heat of dilution value while performing heat and mass transfer analyses of these potential non-conventional working fluid mixtures in absorption cooling systems.

Nomenclature:

a, b, c	constants
H	enthalpy (kJ kg^{-1})
i	i^{th} term
m	slope
P	pressure (Pa)
T	temperature (K)
V	volume ($\text{m}^3 \text{kg}^{-1}$)
w	mass fraction
y	y-coordinate intercept

Superscripts:

s	solution
sup	superheated
sat	saturated
w	water

Subscripts:

d	dilution
f	liquid state
v	vapour state

Chemical formulas:

H_2O	water
KNO_3	potassium nitrate
LiBr	lithium bromide
LiCl	lithium chloride
LiI	lithium iodide
LiNO_3	lithium nitrate
NaNO_3	sodium nitrate

1. Introduction

Absorption air-conditioning systems driven by solar thermal energy are gaining global acceptance for space cooling in summer due to their potential to utilize the free solar thermal energy efficiently. Working fluid mixtures employed in the absorption air-conditioning systems are environmental friendly and do not contribute to greenhouse gas emissions unlike vapour compression systems which also use costly mechanical energy input. Intensive research has been carried out to improve the performance and thermal efficiency of absorption air-conditioning systems by adopting suitable operating conditions and improved design and configuration of the components. In commercial absorption air-conditioning systems, water/LiBr is mainly employed as a working fluid mixture and offers outstanding features such as the non-volatility of LiBr absorbent and high heat of vaporization of water. However, water/LiBr based absorption air-conditioning systems suffer from corrosion problems and exhibit a high risk of crystallization when operated at air-cooled thermal conditions. At high cooling-water temperatures and high concentrations, the solution is prone to crystallization. In addition, because of the risk of crystallization, corrosion problems and thermal instability at higher temperatures, water/LiBr working fluid mixture limits the use of high temperature heat sources in triple-effect cycles which are intended to improve the thermal utilization and increase the coefficient of performance of absorption air-conditioning systems. In view of the above mentioned problems associated with water/LiBr working fluid mixture, new working fluid mixtures have been investigated to overcome with the problems associated with the conventional working fluid mixture.

The addition of other salts to water/LiBr can improve the solubility of the solution. Bourouis et al. [1, 2] and Medrano et al. [3] investigated and recommended the use of an aqueous multi-component salt solution ($\text{LiBr} + \text{LiI} + \text{LiNO}_3 + \text{LiCl}$) with mass

compositions in salts of 60.16%, 9.55%, 18.54% and 11.75%, respectively, as a potential absorbent with water as a refrigerant. The multi component salt solution exhibits higher solubility and also reduces the risk of crystallization. Bourouis et al. [1] reported that the presence of lithium chloride decreases the vapour pressure, both lithium iodide and lithium nitrate improve the solubility and lithium nitrate reduces corrosion in the system. The safety margin for crystallization is much higher as its crystallization temperature is about 30 K lower than that of water/LiBr. Thus, the use of the multi-salt working fluid mixture can not only mitigate the problems associated with the conventional water/LiBr working fluid mixture but can also enhance the performance of an absorber operating at air-cooled thermal conditions.

Similarly, as water/LiBr cannot be used in triple-effect cycles driven by high temperature heat sources (above 180 °C) due to corrosion problems and thermal instability, investigations are being performed on the development of potential absorbents that are non-corrosive and thermally stable at higher temperatures so as to efficiently utilize the thermal potential of high temperature heat sources. Aqueous (lithium, potassium, sodium) nitrate solution (Alkitrane) has been suggested as a working fluid in the high temperature stage of a triple-effect cycle [4 - 7]. The working fluid mixture is composed of water as a refrigerant and a ternary salt mixture of lithium nitrate, potassium nitrate and sodium nitrate as an absorbent with a mass composition in salts of 53%, 28% and 19%, respectively. The use of an Alkitrane solution can be potentially useful in applications in which the available heat source temperature is very high because it is non-corrosive and has high thermal stability up to a temperature of about 260 °C.

The aqueous multi-component salt solution ($\text{LiBr} + \text{LiI} + \text{LiNO}_3 + \text{LiCl}$) and aqueous (lithium, potassium, sodium) nitrate solution can be considered as promising

alternatives to the conventional water/LiBr working fluid mixture to enhance the performance of absorption air-conditioning systems operating at air-cooled thermal conditions and high temperature heat source conditions, respectively.

Many researchers have investigated the thermophysical properties of these non-conventional working fluids such as vapour pressure, density, viscosity, specific heat, thermal conductivity etc. Although thermodynamic simulations have been performed with these non-conventional working fluid mixtures to investigate the cycle performance, there is very scarce information in the literature about the absorption and desorption processes. Heat and mass transfer phenomena which simultaneously occur in the absorber and desorber of an absorption air-conditioning system have to be investigated in order to evaluate the performance of the component. In many numerical approaches for analysis of heat and mass transfer phenomena in an absorber the differential heat of dilution is an important property to be known. Differential heat of dilution is the heat which evolves when a unit weight of solvent is added to an infinite weight of solution at a constant temperature and concentration. In the absorber of an absorption air-conditioning system, when the refrigerant is absorbed in the solution, heat evolves as a result of mixing and condensation and is known as heat of absorption. The heat of absorption is calculated from the enthalpies of the liquid state and vapour state and the differential heat of dilution. Therefore, differential heat of dilution is needed in the numerical modelling of heat transfer in the absorber. However, the differential heat of dilution data of the above non-conventional working fluid mixtures are not known.

Although differential heat of dilution can be determined experimentally using a calorimeter, another way is to estimate the differential heat of dilution from the enthalpy-concentration charts or vapour pressure data. Analytical method of calculating

differential heat of dilution is simple and easy as the vapour pressure data of the examined working fluid mixtures is available. Brown [8] described that the Clapeyron equation for a liquid substance and a solution containing that liquid as a solvent can be combined to derive a relation in which the differential term represents the slope of the Duhring line. Haltenberger [9] reported that the slopes of the Duhring lines are constant at low concentrations and vary slightly at higher concentrations. He explained that an exact relation is obtained using the Clapeyron equation, which is applicable to all systems containing a single volatile constituent. The author used the vapour pressure of sodium hydroxide solutions to construct a Duhring chart from which he calculated the enthalpy of solution. The calculated values of differential heat of dilution using experimental data of heat capacity were used to construct an enthalpy-concentration chart. A similar approach was followed by McNeely [10] who derived the differential heat of dilution data of water/LiBr theoretically from the Duhring's diagram using the Clapeyron equation. In this work, a similar theoretical procedure has been adopted to calculate the differential heat of dilution from the Duhring's diagram, however a new database for the vapour pressure calculation of water/LiBr is used. Further, a polynomial correlation has been derived for the calculation of the differential heat of dilution value for a range of concentration at different temperatures. The analytically calculated data obtained for water/LiBr were validated against the experimental data available in the literature and are found well in agreement with the experimental values. Further, the same procedure is used to estimate the differential heat of dilution of the multi-component salt aqueous solution ($\text{LiBr} + \text{LiI} + \text{LiNO}_3 + \text{LiCl}$) and aqueous (lithium, potassium, sodium) nitrate solution and the data were correlated using a polynomial equation as a function of temperature and concentration. The obtained correlations to calculate the differential heat of dilution could be useful in performing a

heat and mass transfer analysis of these non-conventional working fluid mixtures in the components of absorption cooling systems.

2. Calculation Methodology

The Clausius-Clapeyron equation which is used for characterizing a discontinuous phase transition between two phases of matter of a single constituent can be written in a differential form as:

$$\frac{dP}{dT} = \frac{\Delta H}{\Delta V T} \quad (1)$$

Applying the Clausius-Clapeyron equation for the refrigerant which is water and the absorbent which is an aqueous solution of salt or mixture of salts, we obtain:

$$\frac{dP^w}{dT^w} = \frac{\Delta H^w}{\Delta V^w T^w} \quad (2)$$

and

$$\frac{dP^s}{dT^s} = \frac{\Delta H^s}{\Delta V^s T^s} \quad (3)$$

where, the superscript w denotes water and s denotes solution. T is the absolute saturation temperature in K, P is the saturation pressure in Pa, ΔH is the latent heat at temperature T and pressure P in kJ kg^{-1} and ΔV is the difference between vapour and liquid volumes in $\text{m}^3 \text{kg}^{-1}$.

For the same water vapour pressure, when $P^w = P^s$, dividing equation 2 by equation 3, we obtain:

$$\frac{dT^s}{dT^w} = \frac{\Delta H^w \Delta V^s T^s}{\Delta H^s \Delta V^w T^w} \quad (4)$$

As the liquid volume is negligible in comparison with its volume in the vapour phase, therefore, ΔV can be replaced by the vapour volume.

$$\frac{dT^s}{dT^w} = \frac{\Delta H^w V^{\text{sup}} T^s}{\Delta H^s V^{\text{sat}} T^w} \quad (5)$$

where V^{sat} is the volume of saturated water vapour and V^{sup} is the volume of superheated water vapour at saturation temperature of the solution. The degree of superheat is equal to $T^s - T^w$. Equation 5 represents the Duhring equation derived from the Clausius-Clapeyron equation.

According to Duhring's rule, if the boiling point of the solution is plotted against the boiling point of its solvent at the same pressure, the resultant plot will be a straight line.

The equation of a straight line can be represented as:

$$T^s = mT^w + y \quad (6)$$

where m is the slope of the line and y is the y-coordinate intercept.

by differentiating equation (6), we obtain:

$$\frac{dT^s}{dT^w} = m \quad (7)$$

Similarly the Duhring equation can be represented by an equation of a straight line where m and y are constants for any given concentration.

$$\frac{dT^s}{dT^w} = \frac{\Delta H^w V^{\text{sup}} T^s}{\Delta H^s V^{\text{sat}} T^w} = m \quad (8)$$

The slope m of each line for each concentration is calculated from the Duhring's diagram. Saturation temperature of water vapour, specific volume of saturated water

vapour and super heated water vapour are calculated from the steam table. Latent heat of water ΔH^w is given as:

$$\Delta H^w = H_v^w - H_f^w \quad (9)$$

where H_v^w is the saturated water vapour enthalpy and H_f^w is the saturated water enthalpy at temperature T^w . All values in equation 8 are known except ΔH^s . By rearranging equation 8 we get:

$$\Delta H^s = \frac{\Delta H^w V^{\text{sup}} T^s}{mV^{\text{sat}} T^w} \quad (10)$$

The differential heat of dilution is given as:

$$H_d = \bar{H} - H_f \quad (11)$$

where H_f is the enthalpy of water at temperature T^s and \bar{H} is the partial enthalpy of water and is given as:

$$\bar{H} = H_v - \Delta H^s \quad (12)$$

where H_v is the superheated water vapour enthalpy at temperature T^s . By substituting the variables, the differential heat of dilution can be expressed as:

$$H_d = H_v - \frac{\Delta H^w V^{\text{sup}} T^s}{mV^{\text{sat}} T^w} - H_f \quad (13)$$

By substituting all the values in equation 13, the differential heat of dilution is calculated for different solution concentration at different temperature.

3. Vapour Pressure Data

Vapour liquid equilibria of all the working fluid mixtures were taken from the recent available experimental data. The correlation developed by Patek and Klomfar [11] to calculate the thermodynamic properties of water/LiBr was used to calculate the saturation temperature of the water/LiBr solution. The vapour pressure data of Koo et al. [12] and the correlation developed by the research group CREVER from Rovira i Virgili University [13] were used to calculate the saturation temperature of the quaternary salt working fluid mixture. To calculate the saturation temperature of the solution of Alkilate, the correlation developed by Álvarez et al. [14] was used. The thermodynamic properties of water were calculated using the IAPWS formulation 1995 reported by Wagner and Pruß [15].

4. Validation

Differential heat of dilution was theoretically calculated for water/LiBr solution using the above procedure and thermophysical properties and the data obtained were validated against the experimental data of Uemura et al. [16], Lange and Schwartz [17] and Feuerecker et al. [18]. As the differential heat of dilution data reported in the literature is measured at 25 °C therefore, in the derived polynomial correlation the temperature is kept constant at 25°C. Figure 1 shows the comparison of the analytically estimated and experimentally reported data. The estimated result is well in agreement with the experimental data with an absolute mean percentage error of 5.46%.

5. Results and Discussion

The differential heat of dilution is theoretically calculated for all the three working fluid mixtures considered in the present work for a range of concentrations at different temperatures and covering the typical operating conditions of each working fluid mixture in absorption cooling systems. The saturation temperature of the solution was plotted against the saturation temperature of the water at the same pressure. The procedure was repeated for different solution concentrations of interest for absorption cooling cycles operating with the three working fluid mixtures. For each solution concentration, a straight line was obtained and the slope of the line was calculated. The slope m of the straight line at a given concentration, solution temperatures and corresponding dew point temperatures for water/LiBr, water/(LiBr+LiI+LiNO₃+LiCl) and water/(LiNO₃+KNO₃+NaNO₃) are tabulated in Table 1, 2 and 3, respectively. The slope of each line was used to calculate the differential heat of dilution for the given concentration of solution at different temperatures. Figures 2, 3 and 4 show the variation of the differential heat of dilution as a function of temperature and concentration. Figures 2 and 3 show that the differential heat of dilution increases significantly with an increase in solution concentration; however, a slight increase is observed with an increase in temperature at a given concentration of the solution. It can be seen from Figure 3 that the differential heat of dilution varies linearly with temperature in case of lower absorbent concentration. Whereas, in case of higher absorbent concentration no significant increase in the differential heat of dilution is observed with increase in temperature initially in the range of 298 – 320 K, however, a significant increase in the differential heat of dilution is observed above 320 K. It shows that the increase in the differential heat of dilution is less prominent at higher solution concentration and lower temperatures. In addition, it is worth noting that the differential heat of dilution of the

non-conventional working fluid mixtures, water/(LiBr+LiI+LiNO₃+LiCl) and water/(LiNO₃+KNO₃+NaNO₃), at a given concentration and temperature of interest for absorption cooling cycles is lower than that of the water/LiBr solution, which results in a lower contribution to the heat of absorption. This makes these working fluid mixtures more appropriate for the absorption process taking place in the absorber which is the main component in absorption cooling systems. The estimated differential heat of dilution data for each working fluid mixture was correlated with the simple polynomial equation given below

$$H_d = \sum_{i=0}^3 [(a_i + b_i T + c_i T^2) w^i] \quad (14)$$

Equation 14 represents the correlation to estimate the differential heat of dilution of each working fluid mixture as a function of concentration and temperature. In the above correlation T represents temperature in K and w represents concentration of the absorbent in mass fraction. The values of the regressed parameters in the equation are tabulated in Table 4 for each working fluid mixture. The correlation is able to predict the differential heat of dilution with a mean absolute percentage error of 0.54%, 0.70% and 1.66% for water/LiBr, water/(LiBr+LiI+LiNO₃+LiCl) and water/(LiNO₃+KNO₃+NaNO₃), respectively. The correlation is valid for a concentration range of 45–65%, 55–67% and 60–85% and a temperature range of 20–50 °C, 25–60 °C and 80–150 °C for water/LiBr, water/(LiBr+LiI+LiNO₃+LiCl) and water/(LiNO₃+KNO₃+NaNO₃), respectively. The concentration ranges for the validity of the correlations depend on the use of the examined fluid mixtures. In this paper, the concentration and temperature ranges are taken in context of absorption cooling applications. The examined fluid mixtures are considered potential working pairs in absorption cooling systems. As this work is intended to estimate the differential heat of

dilution which is used in the heat transfer calculation in the absorber of absorption cooling systems, the selection of composition and temperature ranges in the calculation are based on the typical operating conditions of these systems employing the examined working fluid mixtures.

6. Conclusion

The differential heat of dilution, which contributes in the heat evolved during the absorption process, is required in many numerical approaches to analyse the heat and mass transfer phenomena. The differential heat of dilution of water/lithium bromide, water/(lithium bromide+lithium iodide +lithium nitrate+lithium chloride) with mass compositions in salts of 60.16%, 9.55%, 18.54% and 11.75%, respectively, and water/(lithium nitrate+potassium nitrate+sodium nitrate) with mass compositions in salts of 53%, 28% and 19%, respectively was analytically calculated in this paper. The analytical procedure to estimate the differential heat of dilution from the Dühring's diagrams using the vapour pressure data is an interesting alternative to experimental techniques, as the analytically calculated values are well in agreement with the experimental values. In this study, the Clausius-Clapeyron equation was used to derive the Dühring equation and using the vapour pressure data of the examined mixtures, the differential heat of dilution data were estimated from the Dührings diagrams. The differential heat of dilution data obtained were correlated with simple polynomial equations for the three working fluids as a function of the solution concentration and temperature. The correlation is able to predict the differential heat of dilution with a mean absolute percentage error of 0.54%, 0.70% and 1.66% for water/LiBr, water/(LiBr+LiI+LiNO₃+LiCl) and water/(LiNO₃+KNO₃+NaNO₃), respectively. The results showed that the differential heat of dilution of the non-conventional working fluid mixtures is lower than that of water/LiBr at typical operating temperature and

concentration of interest in absorption cooling cycles employing these working fluid mixtures. For instance, the differential heat of dilution of water/LiBr at typical operating conditions lies in the range of 300 – 400 kJ kg⁻¹ whereas the differential heat of dilution of the quaternary working fluid and Alktrate solution lies in the range of 250 – 350 kJ kg⁻¹ and 200 – 300 kJ kg⁻¹, respectively, at typical operating conditions of these working fluid mixtures. Therefore it is concluded that the performance of the absorber could be improved with these non-conventional working fluid mixtures because of the lower heat of absorption. Reduction in the heat of absorption released at the solution vapour interface allows for a reduction in the partial pressure of water vapour in the solution at the interface, consequently increasing the absorption capability of the solution. The correlations developed could be useful in predicting the differential heat of dilution value while performing heat and mass transfer analyses of these potential non-conventional working fluid mixtures in the absorption process of absorption cooling systems.

Acknowledgements

Faisal Asfand gratefully acknowledges the Rovira i Virgili University for granting the Martí-Franquès research fellowship 2012 (2012BPURV-50) to pursue a doctorate degree.

References

1. Bourouis M, Vallès M, Medrano M, Coronas A. Absorption of water vapour in the falling film of water-(LiBr+LiI+LiNO₃+LiCl) in a vertical tube at air-cooling thermal conditions. *International Journal of Thermal Sciences*. 2005; 44:491–8.
2. Bourouis M, Vallès M, Medrano M, Coronas A. Performance of air-cooled absorption air conditioning systems working with water-(LiBr+LiI+LiNO₃+LiCl). *Journal of Process Mechanical Engineering*. 2005; 219:205–12.
3. Medrano M, Bourouis M, Coronas A. Absorption of water vapour in the falling film of water-lithium bromide inside a vertical tube at air-cooling thermal conditions. *International Journal of Thermal Science*. 2002; 41:891–8.
4. Davidson W, Erickson D. 260 °C Aqueous absorption working pair under development. *Newsl. IEA Heat Pump Cent*. 1986; 4:29–31.
5. Howe L, Erickson D. Proof-of-Concept Testing of Alkiltrate. Phase III. Final Report-Energy Concepts Co. 1990. USA.
6. Erickson D, Potnis SV, Tang J. Triple Effect Absorption Cycles. *Energy Conversion Engineering Conference IECEC 96. Proceedings of The 31st Intersociety*. 1996; 1072–7.
7. Álvarez ME, Esteve X, Bourouis M. Performance analysis of a triple-effect absorption cooling cycle using aqueous (lithium, potassium, sodium) nitrate solution as a working pair. *Applied Thermal Engineering*. 2015; 79:27–36.
8. Brown GG. Solution cycles as applied to set-up transformers for temperatures. *Journal of the Franklin Institute*. 1935; 219:405–32.
9. Haltenberger W. Enthalpy-concentration charts from vapor pressure data. *Industrial and Engineering Chemistry*. 1939; 31:783–6.
10. McNeely NA. Thermodynamics properties of aqueous solutions of lithium bromide. *ASHRAE Transactions*. 1979; 85:413–34.
11. Patek J, Klomfar J. A computationally effective formulation of the thermodynamic properties of LiBr-H₂O from 273 to 500 K over full composition range. *Int. J. of Refrigeration*. 2006; 29:566–78.
12. Koo KK, Lee HR, Jeong S, Oh YS, Park DR, Baek YS. Solubilities, Vapor Pressures, and Heat Capacities of the Water + Lithium Bromide + Lithium Nitrate + Lithium Iodide + Lithium Chloride System. *International Journal of Thermophysics*. 1999; 20:589–600.
13. Confidential Report. Thermophysical properties of the fluid mixture water/(LiBr+LiI+LiNO₃+LiCl). *Universitat Rovira i Virgili*. 2012.

14. Álvarez ME, Bourouis M, Esteve X. Vapor-liquid equilibrium of aqueous alkaline nitrate and nitrite solutions for absorption refrigeration cycles with high temperature driving heat. *Journal of Chemical & Engineering Data*. 2011; 56:491–6.
15. Wagner W, Pruß A. The IAPWS Formulation 1995 for the Thermodynamic Properties of Ordinary Water Substance for General and Scientific Use. *Journal of Physical and Chemical Reference Data*. 2002; 31:387–535.
16. Uemura T, Hasaba S. Studies on the lithium bromide-water absorption refrigeration machine. *Technology Reports of Kansai University*. 1964; 6:31–55.
17. Lange E, Schwartz E. Lösungs and verdünnungswärmen von salzen von äussersten verdünnung bis zur sättigung-IV Lithiumbromid. *Z. Physikal. Chem.* 1928; 133:129–50.
18. Feuerecker G, Scharfe J, Greiter I, Frank C, Alefeld G. Measurement of thermophysical properties of aqueous LiBr-solutions at high temperatures and concentrations. *Proc. International Absorption Heat Pump Conf. ASME*. 1993; 31:493–9.

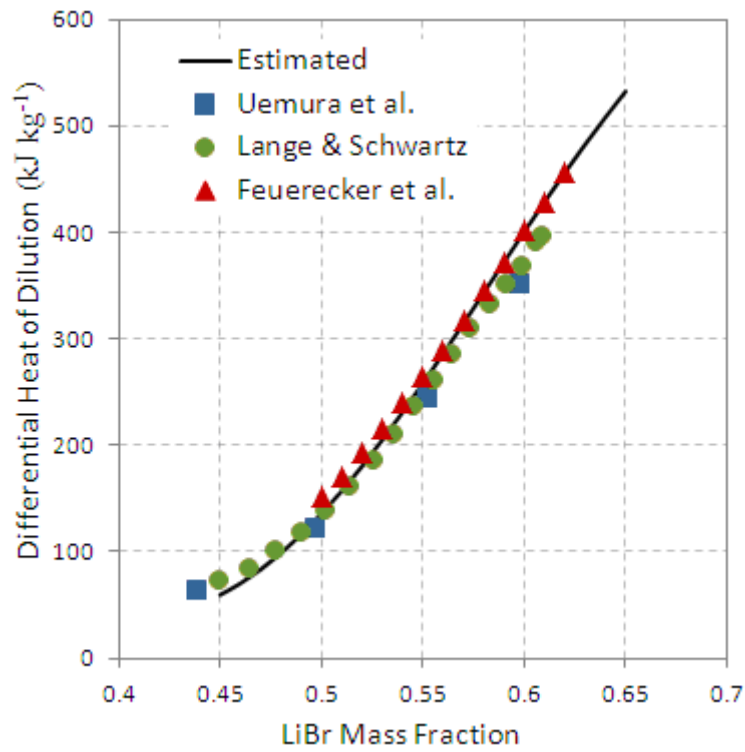


Figure 1: Validation of differential heat of dilution for water/LiBr at 25 °C

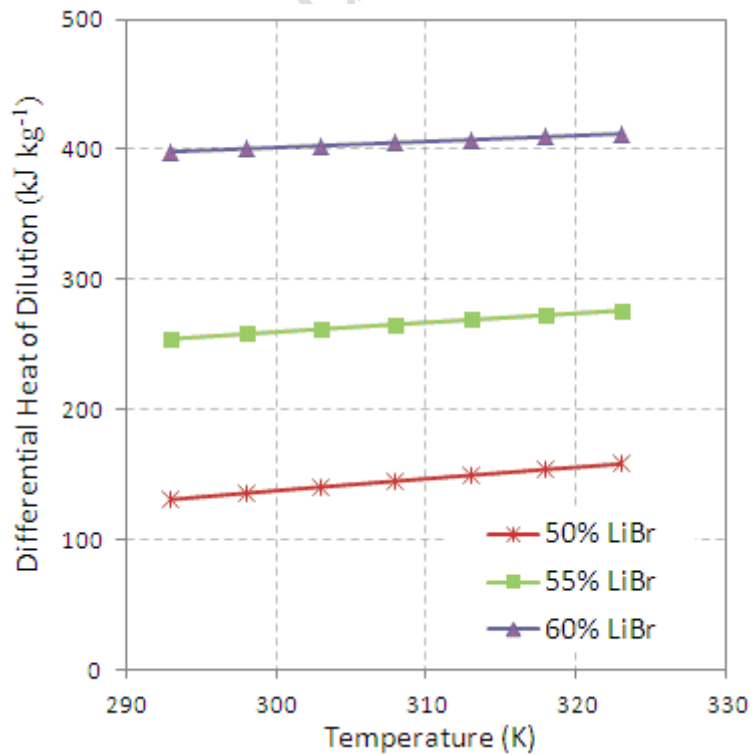


Figure 2: Differential heat of dilution for water/LiBr working fluid

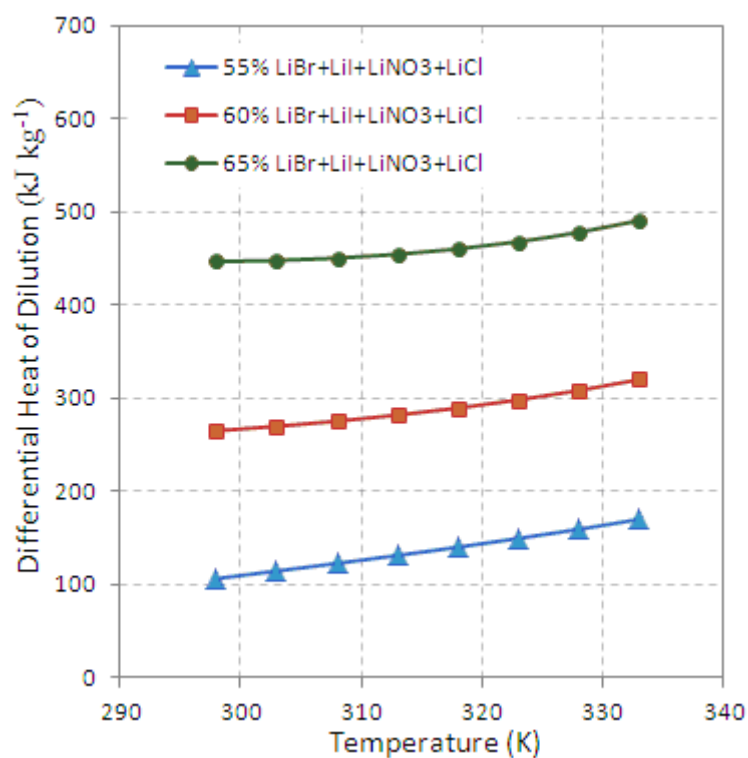


Figure 3: Differential heat of dilution for water/(LiBr+LiI+LiNO₃+LiCl) working fluid

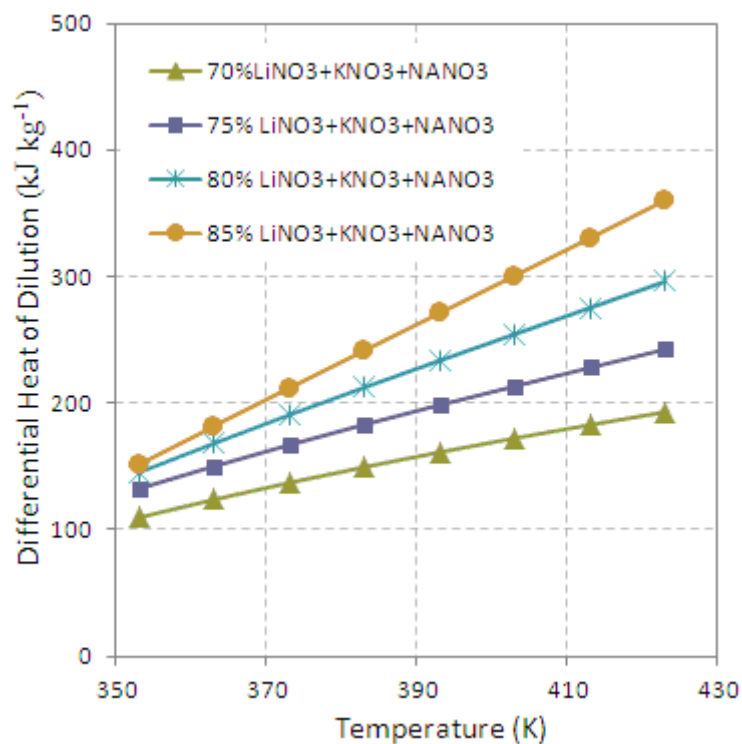


Figure 4: Differential heat of dilution for water/(LiNO₃+KNO₃+NaNO₃) working fluid

Table 1: Dew point and solution temperatures of the water/LiBr solution at different concentrations with the corresponding slope of the line on the Duhring's Diagram

Absorbent Mass Fraction	Slope m	Solution Temperature (°C)							
		20	40	60	80	100	120	140	160
		Corresponding Dew Point Temperature (°C)							
0.45	1.1013	5.90	24.06	42.22	60.39	78.55	96.71	114.90	133.00
0.46	1.1056	4.84	22.93	41.01	59.10	77.18	95.27	113.40	131.40
0.47	1.1104	3.71	21.72	39.73	57.75	75.76	93.77	111.80	129.80
0.48	1.1153	2.52	20.45	38.39	56.33	74.27	92.20	110.10	128.10
0.49	1.1194	1.25	19.11	36.98	54.85	72.71	90.58	108.40	126.30
0.50	1.1238	-0.09	17.71	35.51	53.31	71.10	88.90	106.70	124.50
0.51	1.1279	-1.49	16.24	33.98	51.71	69.44	87.17	104.90	122.60
0.52	1.1321	-2.95	14.72	32.39	50.05	67.72	85.39	103.10	120.70
0.53	1.1360	-4.47	13.14	30.74	48.35	65.96	83.57	101.20	118.80
0.54	1.1399	-6.04	11.51	29.06	46.60	64.15	81.70	99.25	116.80
0.55	1.1433	-7.65	9.84	27.33	44.82	62.31	79.80	97.29	114.80
0.56	1.1473	-9.29	8.14	25.57	43.00	60.43	77.86	95.29	112.70
0.57	1.1511	-10.97	6.41	23.78	41.15	58.53	75.90	93.27	110.60
0.58	1.1551	-12.65	4.66	21.98	39.29	56.60	73.92	91.23	108.50
0.59	1.1595	-14.34	2.91	20.16	37.41	54.66	71.91	89.17	106.40
0.60	1.1637	-16.03	1.15	18.34	35.53	52.71	69.90	87.09	104.30
0.61	1.1684	-17.71	-0.59	16.52	33.64	50.76	67.87	84.99	102.10
0.62	1.1737	-19.36	-2.32	14.72	31.76	48.80	65.84	82.88	99.91
0.63	1.1795	-20.97	-4.02	12.93	29.89	46.84	63.80	80.75	97.71
0.64	1.1859	-22.55	-5.69	11.17	28.03	44.89	61.75	78.61	95.47
0.65	1.1934	-24.08	-7.33	9.43	26.19	42.95	59.70	76.46	93.22

Table 2: Dew point and solution temperatures of the water/(LiBr+LiI+LiNO₃+LiCl) solution at different concentrations with the corresponding slope of the line on the Duhring's Diagram

Absorbent Mass Fraction	Slope m	Solution Temperature (°C)							
		30	40	60	80	100	120	140	160
		Corresponding Dew Point Temperature (°C)							
0.55	1.1879	4.30	12.82	29.83	46.63	63.03	82.65	101.30	120.10
0.56	1.1889	2.69	11.25	28.30	45.10	61.46	80.71	99.09	117.60
0.57	1.1899	1.02	9.61	26.71	43.53	59.86	78.64	96.77	115.00
0.58	1.1910	-0.62	7.92	25.07	41.92	58.23	76.50	94.42	112.40
0.59	1.1921	-2.21	6.16	23.38	40.26	56.57	74.30	92.07	109.90
0.60	1.1934	-3.84	4.36	21.63	38.56	54.88	72.07	89.77	107.50
0.61	1.1945	-5.53	2.50	19.84	36.82	53.17	69.85	87.55	105.30
0.62	1.1958	-7.26	0.59	18.00	35.04	51.43	67.66	85.41	103.30
0.63	1.1969	-9.05	-1.21	16.12	33.23	49.66	65.52	83.36	101.30
0.64	1.1981	-10.87	-2.97	14.20	31.38	47.87	63.44	81.39	99.49
0.65	1.1991	-12.74	-4.79	12.24	29.50	46.07	61.45	79.50	97.72
0.66	1.2003	-14.65	-6.63	10.25	27.59	44.24	59.56	77.65	95.94
0.67	1.2013	-16.59	-8.52	8.22	25.66	42.39	57.78	75.82	94.07

Table 3: Dew point and solution temperatures of the water/(LiNO₃+KNO₃+NaNO₃) solution at different concentrations with the corresponding slope of the line on the Duhring's Diagram

Absorbent Mass Fraction	Slope m	Solution Temperature (°C)							
		70	80	90	100	110	120	130	140
		Corresponding Dew Point Temperature (°C)							
0.6	1.1118	54.69	63.51	72.37	81.26	90.18	99.14	108.10	117.20
0.65	1.1240	51.07	59.78	68.53	77.31	86.12	94.96	103.80	112.80
0.7	1.1505	46.85	55.38	63.92	72.49	81.09	89.72	98.38	107.10
0.75	1.1931	41.86	50.10	58.37	66.64	74.94	83.26	91.60	99.96
0.76	1.2036	40.79	48.97	57.17	65.38	73.60	81.85	90.11	98.40
0.77	1.2150	39.69	47.81	55.94	64.08	72.23	80.40	88.59	96.80
0.78	1.2272	38.58	46.63	54.69	62.75	70.83	78.92	87.03	95.15
0.79	1.2403	37.44	45.42	53.40	61.40	69.40	77.41	85.43	93.47
0.8	1.2544	36.28	44.19	52.10	60.01	67.93	75.86	83.80	91.75
0.81	1.2692	35.10	42.94	50.77	58.60	66.44	74.28	82.13	89.99
0.82	1.2851	33.91	41.66	49.42	57.17	64.92	72.67	80.43	88.19
0.83	1.3019	32.69	40.37	48.04	55.71	63.37	71.03	78.70	86.37
0.84	1.3200	31.46	39.05	46.64	54.22	61.80	69.37	76.94	84.51
0.85	1.3392	30.21	37.72	45.22	52.71	60.20	67.67	75.15	82.62
0.86	1.3595	28.94	36.37	43.78	51.18	58.57	65.96	73.33	80.70
0.87	1.3812	27.65	35.00	42.32	49.63	56.93	64.21	71.49	78.75
0.88	1.4042	26.35	33.61	40.85	48.06	55.26	62.45	69.62	76.78
0.89	1.4287	25.04	32.21	39.35	46.47	53.57	60.66	67.73	74.78
0.9	1.4548	23.71	30.79	37.84	44.86	51.87	58.85	65.81	72.76
0.95	1.6129	16.77	23.38	29.95	36.48	42.98	49.44	55.86	62.25

Table 4: Regressed values of the coefficients in equation 14

	a_i	b_i	c_i
Water/LiBr working fluid			
i=0	0.992786	-3.80487	0.06707
i=1	1.017947	-0.3167	-0.31698
i=2	1.06683	12.75037	0.548797
i=3	1.044128	6.897941	-0.35639
Water/(LiBr+LiI+LiNO₃+LiCl) working fluid			
i=0	0.932142	-8.91989	0.053392
i=1	1.032266	6.815861	-0.17187
i=2	1.062847	9.656643	0.229848
i=3	1.063738	7.55447	-0.14364
Water/(LiNO₃+KNO₃+NaNO₃) working fluid			
i=0	1.005307	-8.70613	0.016192
i=1	0.841477	19.01825	-0.02999
i=2	0.692006	0.003384	-0.0169
i=3	0.5949	-14.7523	0.044434